Spin Polarization and Transport of Surface States in the Topological Insulators Bi_2Se_3 and Bi_2Te_3 from First Principles

Oleg V. Yazyev, Joel E. Moore, and Steven G. Louie

Department of Physics, University of California, Berkeley, California 94720, USA

Materials Sciences Division, Lawrence Berkeley National Laboratory, Berkeley, California 94720, USA

(Received 29 August 2010; revised manuscript received 27 October 2010; published 29 December 2010)

We investigate the band dispersion and the spin texture of topologically protected surface states in the bulk topological insulators Bi_2Se_3 and Bi_2Te_3 by first-principles methods. Strong spin-orbit entanglement in these materials reduces the spin polarization of the surface states to ~50% in both cases; this reduction is absent in simple models but of important implications to essentially any spintronic application. We propose a way of controlling the magnitude of spin polarization associated with a charge current in thin films of topological insulators by means of an external electric field. The proposed dual-gate device configuration provides new possibilities for electrical control of spin.

DOI: 10.1103/PhysRevLett.105.266806 PACS numbers: 73.20.−r, 72.25.−b, 75.70.Tj

The recently discovered three-dimensional topological insulators (TIs) [1–3] realize an unconventional electronic phase driven by strong spin-orbit interaction (SOI). The striking feature of these heavy-element materials is the existence of metallic Dirac fermion surface states characterized by an intrinsic spin helicity: the wave vector of the electron determines its spin state. A net spin density is thus produced upon driving a charge current at the surface of a TI. Considerable effort has been devoted recently to possible applications of this property of TIs to novel electronic devices, e.g., to spintronics [4] and topological quantum computing [5].

Understanding the properties of bulk TIs has mostly relied on few-band phenomenological models which treat the helical surface states as fully spin-polarized. However, one has to keep in mind that SOI entangles the spin and orbital momentum degrees of freedom thus reducing spin polarization. This is especially so for the currently investigated bulk TIs in which SOI is of electron-volt magnitude due to the presence of bismuth, the element with the largest atomic number Z which has stable isotopes [6,7].

In this Letter, we apply first-principles methodology to study the topological surface states in Bi_2Se_3 and Bi_2Te_3, the ''second generation'' materials which are currently considered as reference TIs [8,9]. This approach is free of empirical parameters and treats topological surface states on an equal footing with other states across the electronic spectrum. The degree of spin polarization of the topological surface states is found to be significantly reduced in both bismuth materials, and this reduction will affect most spintronic applications of these materials. We use our results to propose a way of controlling the degree of spin polarization associated with the charge current in thin TI slabs by applying a transverse electric field. The proposed spintronic device is compared to a related proposal based on spin-polarized edge states in graphene [10] and to conventional semiconductor quantum wells.

First-principles electronic structure calculations have been performed within the density functional theory (DFT) framework employing the generalized gradient approximation (GGA) to the exchange-correlation functional [11]. Spin-orbit effects were treated self-consistently using fully relativistic norm-conserving pseudopotentials [12] acting on valence electron wave functions represented in the two-component spinor form [13]. A plane-wave kinetic energy cutoff of 35 Ry has been employed for the wave functions. Surface states in Bi_2Se_3 and Bi_2Te_3 bulk TIs were investigated using (111) slab models of varying thickness [1–5 quintuple layers (QL) equivalent to ~1–5 nm] with atomic positions taken from experimental data using a supercell geometry [14]. Such an approach has already been used previously [8,15,16]. The effects of applied electric field were simulated by adding a sawtoothlike potential profile with a constant slope in the slab region [17]. The PWSCF code of the QUANTUM-ESPRESSO distribution [18] was used in the present study.

We start our discussion by considering the band structure of the bulk materials and slabs of finite thickness. Figure 1(a) shows the band structure of 5 QL slabs superimposed with the bulk band structure projected onto the surface Brillouin zone. The band structures of the slab and bulk systems are aligned by matching the potential in the ''bulklike'' region of the slab to the bulk potential. Within the DFT-GGA approach the band gaps of Bi_2Se_3 and Bi_2Te_3 are 0.31 and 0.08 eV, respectively. The value for Bi_2Se_3 is in good agreement with another theoretical report (0.32 eV [19]) and experimental data (0.35 eV [20]), a fortuitous result considering the well-known tendency of DFT to underestimate band gaps [21]. The calculated band gap for Bi_2Te_3 is consistent with another first-principles result [22] and is smaller than 0.165 eV measured experimentally [23].

The topological surface states are distinguished in the slab band structures as the ''Dirac cone'' feature at the Γ

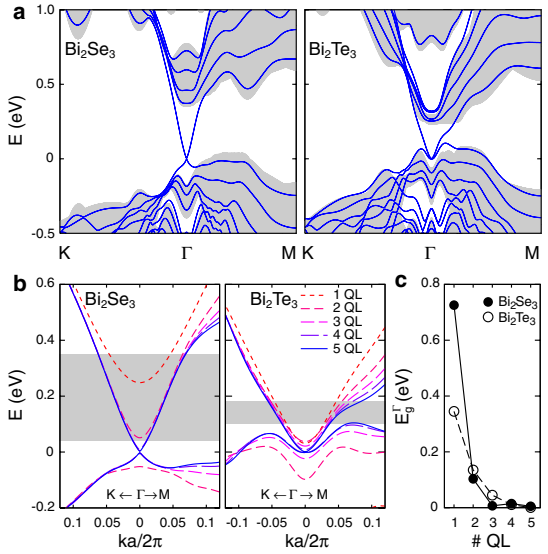

FIG. 1 (color online). (a) Band structure of the 5 QL slabs of Bi_2Se_3 and Bi_2Te_3 (lines) superimposed with the projected band structure of the corresponding bulk materials (shaded areas). (b) Evolution of the surface-state band dispersion in the vicinity of Γ point as a function of slab thickness. Shaded areas show the bulk band gaps. (c) Band gaps at the Γ point induced by the interaction between the surface states as a function of slab thickness.

point, especially clear in the case of Bi_2Se_3. The Dirac point energies E^D (below, $E^D = 0$ eV is set for convenience) are situated 0.04 and 0.10 eV below the corresponding bulk valence band maxima (VBM) within DFT-GGA. In slab geometry, the surface-state bands are doubly degenerate with corresponding surface states of the opposite spin helicities localized at the opposite surfaces. The topological surface bands do not respect electron-hole symmetry. At the VBM energy the calculated Fermi velocity $v_F = 4.6 \times 10^5$ m/s in Bi_2Se_3 agrees with experimental results [8] and shows a moderate dependence on energy. In contrast, strong softening is predicted for Bi_2Te_3 along the Γ-M direction at the conduction band minimum energy. Figure 1(b) illustrates the evolution of the surface band dispersion as a function of slab thickness. Vacuum potential alignment is used for the comparison of the slab systems. In thin slabs, the interactions between the states localized at the opposite surfaces opens a gap (E_g^Γ) at the Dirac point. The magnitude of the gap decays rapidly with increasing slab thickness [Fig. 1(c)], and the values are in quantitative agreement with other first-principles results [15]. The dispersion of the surface-state bands is essentially converged by 3 and 4 QL in Bi_2Se_3 and Bi_2Te_3, respectively.

The striking feature of the surface states of TIs is the helicity of the spin-polarization vector $\vec{P}(\vec{k}) = (2/\hbar) \times [\langle S_x(\vec{k})\rangle, \langle S_y(\vec{k})\rangle, \langle S_z(\vec{k})\rangle]$ along the constant energy contours. Here, the expectation values of spin operators $\langle S_\alpha(\vec{k})\rangle = (\hbar/2)\langle\psi(\vec{k})|\sigma_\alpha|\psi(\vec{k})\rangle$ $(\alpha = x,\ y,\ z)$, where $\psi(\vec{k})$ are the two-component spinor wave functions, σ_α the corresponding Pauli matrices. The recent spin- and angle-resolved photoemission spectroscopy (spin-ARPES) experiments have indeed indicated a one-to-one locking of the momentum and the direction of spin-polarization vector pointing along $(\vec{k} \times \vec{z})$ [24]. First-principles results have confirmed this picture [25]. However, we would like to stress that the magnitude of spin-polarization $\vec{P}(\vec{k})$ can be reduced from the maximum value of 100% since the electron spin quantum number is no longer conserved in systems with SOI [26]. Spin-orbit coupling leads to Bloch states that are not separately spin eigenstates but instead have entanglement between their spin and orbital parts. An illustration of the effects of SOI on the spin projections in the case of bcc iron is given in Ref. [27]. Such effects are expected to be especially pronounced in bismuth materials where the exceptionally strong SOI, of the order of an electron-volt [6,7], would make the surface states a mixture of bulk states from a broad energy range.

Figures 2(a)–2(c) show the calculated expectation values of the spin operators $\langle S_\alpha(\vec{k})\rangle$ for both electron and hole states of the surface band in Bi_2Se_3 and Bi_2Te_3 along x and y directions in momentum space [see Fig. 2(d) for definition]. The surface normal corresponds to the z direction and the standard convention of the right-handed coordinate system applies [Fig. 2(d), inset]. We find that the spin-polarization vectors are aligned preferentially in the xy plane and the helicity is left (right) handed for the conduction or above E^D (valence or below E^D) bands. This is consistent with previous experimental measurements [24] and theoretical calculations [25]. However, the magnitudes of the spin projections are significantly reduced with respect to the nominal value of $\pm\hbar/2$. Close to the Γ point we find ~50%–60% spin polarization for both materials. Its magnitude tends to decrease with increasing energy. The magnitude of spin projections close to the Dirac point appears to be rather insensitive to the slab thickness (not shown here). We have studied the microscopic origin of the reduction of spin polarization and find that the surface Bloch state is a complex superposition of different spin directions on different atoms; hence the reduction of the spin polarization cannot simply be understood in a tight-binding picture built from atomic eigenstates of total angular momentum. A remarkable out-of-plane spin projection $\langle S_z(\vec{k})\rangle$ develops in the Γ-K direction as it was recently ascribed to the hexagonal warping effect [28].

From the point of view of technological applications, an attractive feature of the TI materials is the intrinsic spin polarization of the current carried by the topological surface states. For charge carriers (electrons) moving along the y direction $(k_y > 0)$ the transferred spin polarization (i.e., spin polarization of the current injected through a transparent tunneling barrier) is along the x axis and its geometric average $\langle P_x(E)\rangle = (\pi/4)|\vec{P}(E)|$. We define $\langle P_x(E)\rangle = \frac{\int d\vec{k} v_y(\vec{k}) P_x(\vec{k}) \delta(E - E_{\vec{k}})}{\int d\vec{k} v_y(\vec{k}) \delta(E - E_{\vec{k}})}$, where $v_y(\vec{k})$ is the carrier

velocity along the transport direction. In the discussed materials $\langle P_x(E)\rangle \approx 50\%$ and shows only weak dependence on E, but changes its sign when the character of charge carriers (electrons vs holes) changes. Moreover, in TI films the opposite spin helicities of the charge carriers at the opposite surfaces would result in zero net spin polarization.

We anticipate that improved control over spin transport can be achieved in few-nanometer thick slabs of Bi_2Se_3 and Bi_2Te_3 which can be produced by molecular-beam epitaxy [29,30], vapor deposition [31,32], or exfoliation [33]. Tuning the chemical potential μ in such thin slabs by gating has already been achieved [32]. Similarly to bilayer graphene [34], the TI slabs are characterized by imperfect screening due to the semimetallic nature of the surface states. Thus, in the dual-gate device configuration or by coupling TI thin films to a ferroelectric substrate it is also possible to control splitting $\delta E = E_2^D - E_1^D$ between the Dirac point energies E_1^D and E_2^D of the two surface bands given with respect to the common chemical potential [Fig. 3(a)]. Such splitting of $\sim$0.1 eV produced by the SiC substrate has been reported for Bi_2Se_3 thin films [29]. Close to the Dirac point, the response of a thin TI film of thickness d to an applied electric field $\vec{E}_{\rm ext}$ is expected to be dominated by the bulk screening contribution, $\delta E = |\vec{E}_{\rm ext}|d/\epsilon_{\|}(0)$. The static dielectric constant along c axis $\epsilon_{\|}(0) = 75$ for Bi_2Te_3, probably smaller for Bi_2Se_3 [35]. Figure 3(b) shows the surface-state band dispersion calculated from first principles for a 3 QL slab of Bi_2Se_3 under applied electric field $\vec{E}_{\rm ext}$ resulting in $\delta E = 0.1$ eV (here, $\vec{E}_{\rm ext} = 1.72$ V/nm for the supercell dimension along z axis equal to 4.36 nm). The conical surface-state bands shift rigidly with respect to each other while the bulklike states (not shown) remain practically unaffected by the applied field. Figure 3(c) shows the individual surface-state Sharvin conductances along the y direction (i.e., the number of ballistic channels per device width along x axis given in the units of lattice constant a), $\bar{G}_y^1$ and $\bar{G}_y^2$, and their sum $\bar{G}_y$.

The applied field lifts the semimetallic conductance close to the charge-neutrality point. Note that for both $\delta E = 0.0$ eV and $\delta E = 0.1$ eV there is a 0.006 eV band gap opening at the charge-neutrality point due to the hybridization of the surface states localized on the opposite sides of the thin film. For $E_1^D < \mu < E_2^D$ the charge carriers are electrons (holes) at surface 1 (2). Importantly, in this range of μ the transferred spin polarization along the x direction is of the same sign for both surface conduction channels [Fig. 3(d)]. The total transferred spin polarization $\langle P_x\rangle$ is nonzero in the case of applied electric field. We note that these conditions are away from the symmetric situation that has been argued to lead to exciton conden sation [36]. The magnitude of $\langle P_x\rangle$ can be tuned by changing μ and achieves its maximum value $\langle P_x\rangle = 0.608$ at

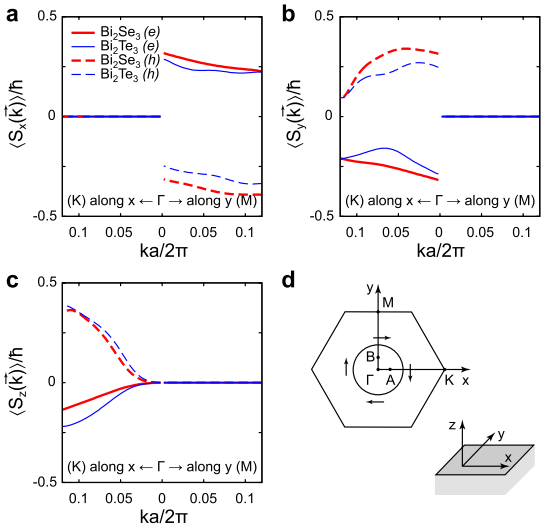

FIG. 2 (color online). (a)–(c) Expectation values of the spin operators $\langle S_\alpha(\vec{k})\rangle$ ($\alpha = x, y, z$) for the topological surface states along the selected path (A-Γ-B) in momentum space (d) for 4 QL slabs of Bi_2Se_3 and Bi_2Te_3. Electron (solid lines) and hole (dashed lines) surface-state bands are distinguished. The surface normal corresponds to the z direction. The coordinate system is right handed [(d), inset].

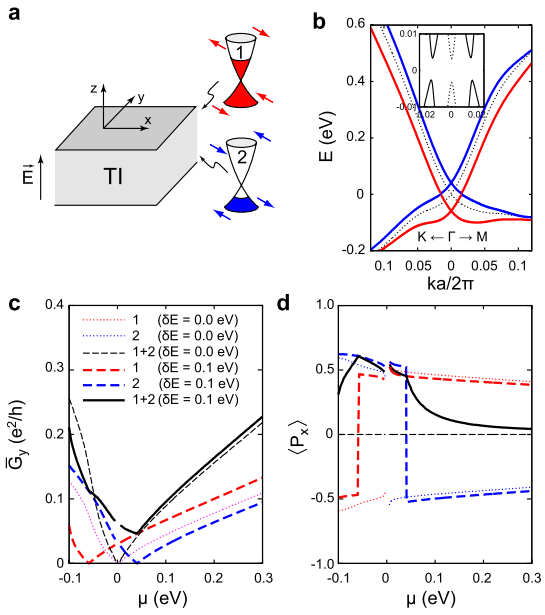

FIG. 3 (color online). (a) Illustration of the effect of electric field $\vec{E}_{\rm ext}$ applied across a thin slab of bulk TI. The filling of the two surface-state bands and the corresponding spin textures for electrons and holes are shown. (b) Splitting of the surface-state bands by applied electric field ($\delta E = 0.1$ eV, solid lines) in a 3QL slab of Bi_2Se_3 compared to the band dispersion at zero field (dotted lines). The inset shows a close-up view of band gaps at the charge-neutrality point. (c) Individual (surfaces 1 and 2) and total ballistic conductances in the y direction per device width $\bar{G}_y$ and (d) spin polarization along the x axis P_x for $\delta E = 0.1$ eV and 0 eV as a function of chemical potential μ ($\mu = 0$ eV corresponds to the charge-neutrality point). The symbols have the same meaning in (c) and (d).

$\mu = E_1^D$. The sign of $\langle P_x \rangle$ can be changed by simply inverting the direction of $\vec{E}_{\text{ext}}$. That is, the dual-gate device based on a thin slab of TI permits to control independently both the conductance and the degree transferred spin polarization of injected current in a broad range, certainly a highly attractive opportunity for spintronics applications.

Such a spintronic device can be compared to another theoretical proposal which realizes electric control over spin transport. This device based on zigzag graphene nanoribbons relies on the peculiar spin-polarized edge states of topologically trivial origin [10]. While in TI slabs the degree of transmitted spin-polarization is limited by the SOI and by the geometric average prefactor $\pi/4$, the localized states at the zigzag edges of graphene are always 100% spin polarized. On the other hand, the degree of spin polarization can be continuously tuned in the TI slabs. The direction of $\vec{P}$ is fixed with respect to the current direction at the TI surfaces, while graphene-based magnetic systems are characterized by low magnetic anisotropy as a result of very weak SOI in carbon and by relatively short spin correlation length [37,38].

In a more general context, it is instructive to compare the spin transport effects at the TI surfaces to those in other 2D systems, e.g., to the corresponding effect induced by Rashba SOI in a 2D electron gas, where a current also induces a spin density. The basic difference is that the Rashba coupling leads to two Fermi surfaces with opposite spin directions at each momentum, and the resulting current-induced spin densities nearly cancel if the SOI is small. A single TI surface has only *one* spin state at each momentum and hence no cancellation. Quantitatively, we write the Rashba SOI as $\alpha\hbar(\vec{k} \times \sigma)_z$ where α has units of velocity and σ are Pauli matrices. The cancellation between Fermi surfaces reduces the spin density by a factor of order α/v_F compared to a model TI surface with a single Dirac cone, where v_F is the Fermi velocity. Taking one example, α in a InGaAs/InAlAs quantum well was measured to be $7–14 \times 10^3$ m/s [39], more than an order of magnitude less than $v_F \sim 5 \times 10^5$ m/s in Bi_2Se_3 and Bi_2Te_3 [8,23].

We would like to thank E. Kioupakis, J. Orenstein, and C. Jozwiak for discussions. This work was supported by NSF Grants No. DMR07-05941 (S. G. L.) and No. DMR08-04413 (J. E. M.) and by the Director, Office of Science, Office of Basic Energy Sciences, Division of Materials Sciences and Engineering Division, U.S. Department of Energy under Contract No. DE-AC02-05CH11231 (O. V. Y.). O. V. Y. received partial support from the Swiss NSF (Grant No. PBELP2-123086). Computational resources have been provided by TeraGrid.

[1] L. Fu, C. L. Kane, and E. J. Mele, Phys. Rev. Lett. **98**, 106803 (2007).
[2] J. E. Moore and L. Balents, Phys. Rev. B **75**, 121306 (2007).
[3] D. Hsieh *et al.*, Nature (London) **452**, 970 (2008).
[4] I. Garate and M. Franz, Phys. Rev. Lett. **104**, 146802 (2010).
[5] L. Fu and C. L. Kane, Phys. Rev. Lett. **100**, 096407 (2008).
[6] P. Carrier and S.-H. Wei, Phys. Rev. B **70**, 035212 (2004).
[7] K. Wittel and R. Manne, Theor. Chim. Acta **33**, 347 (1974).
[8] Y. Xia *et al.*, Nature Phys. **5**, 398 (2009).
[9] H. Zhang *et al.*, Nature Phys. **5**, 438 (2009).
[10] Y.-W. Son, M. L. Cohen, and S. G. Louie, Nature (London) **444**, 347 (2006).
[11] J. P. Perdew, K. Burke, and M. Ernzerhof, Phys. Rev. Lett. **77**, 3865 (1996).
[12] A. Dal Corso and A. Mosca Conte, Phys. Rev. B **71**, 115106 (2005).
[13] L. Nordström and D. J. Singh, Phys. Rev. Lett. **76**, 4420 (1996); T. Oda, A. Pasquarello, and R. Car, Phys. Rev. Lett. **80**, 3622 (1998); R. Gebauer *et al.*, Phys. Rev. B **61**, 6145 (2000).
[14] M. L. Cohen, M. Schlüter, J. R. Chelikowsky, and S. G. Louie, Phys. Rev. B **12**, 5575 (1975).
[15] C.-X. Liu *et al.*, Phys. Rev. B **81**, 041307 (2010); K. Park *et al.*, Phys. Rev. Lett. **105**, 186801 (2010).
[16] S. V. Eremeev, Yu. M. Koroteev, and E. V. Chulkov, Pis'ma Zh. Eksp. Fiz. **91**, 419 (2010) [JETP Lett. **91**, 387 (2010)].
[17] K. Kunc and R. Resta, Phys. Rev. Lett. **51**, 686 (1983); R. Resta and K. Kunc, Phys. Rev. B **34**, 7146 (1986).
[18] P. Giannozzi *et al.*, J. Phys. Condens. Matter **21**, 395502 (2009).
[19] P. Larson *et al.*, Phys. Rev. B **65**, 085108 (2002).
[20] J. Black *et al.*, J. Phys. Chem. Solids **2**, 240 (1957).
[21] M. S. Hybertsen and S. G. Louie, Phys. Rev. B **34**, 5390 (1986).
[22] S. J. Youn and A. J. Freeman, Phys. Rev. B **63**, 085112 (2001).
[23] Y. L. Chen *et al.*, Science **325**, 178 (2009).
[24] D. Hsieh *et al.*, Nature (London) **460**, 1101 (2009).
[25] W. Zhang, R. Yu, H.-J. Zhang, X. Dai, and Z. Fang, New J. Phys. **12**, 065013 (2010).
[26] C. L. Kane and E. J. Mele, Phys. Rev. Lett. **95**, 146802 (2005).
[27] X. Wang, J. R. Yates, I. Souza, and D. Vanderbilt, Phys. Rev. B **74**, 195118 (2006).
[28] L. Fu, Phys. Rev. Lett. **103**, 266801 (2009).
[29] Y. Zhang *et al.*, Nature Phys. **6**, 584 (2010).
[30] Y.-Y. Li *et al.*, Adv. Mater. **22**, 4002 (2010).
[31] D. Kong *et al.*, Nano Lett. **10**, 329 (2010).
[32] D. Kong *et al.*, Nano Lett. **10**, 2245 (2010).
[33] D. Teweldebrhan, V. Goyal, and A. A. Balandin, Nano Lett. **10**, 1209 (2010).
[34] Y. Zhang *et al.*, Nature (London) **459**, 820 (2009).
[35] The Landolt-Börnstein database, http://www.springermaterials.com/
[36] B. Seradjeh, J. E. Moore, and M. Franz, Phys. Rev. Lett. **103**, 066402 (2009).
[37] O. V. Yazyev and M. I. Katsnelson, Phys. Rev. Lett. **100**, 047209 (2008).
[38] O. V. Yazyev, Rep. Prog. Phys. **73**, 056501 (2010).
[39] J. Nitta, T. Akazaki, H. Takayanagi, and T. Enoki, Phys. Rev. Lett. **78**, 1335 (1997).